New Late Middle to Early Upper Ordovician U-Pb zircon ages of extension-related felsic volcanism in the Eastern Pyrenees (NE Iberia): Tectonic implications. .

.

Journal:	*Geological Magazine*
Manuscript ID	GEO-17-1879.R5
Manuscript Type:	Original Article
Date Submitted by the Author:	02-Feb-2019
Complete List of Authors:	Marti, Joan; Geohazards Solari, Luigi; Universidad Nacional Autónoma de México, Centro de Geociencias Casas, Josep Maria; Universitat de Barcelona, Geodinamica i Geofisica Chichorro, Martim; Universidade Nova de Lisboa, GEOBIOTEC, FCT
Keywords:	Upper Ordovician volcanism, Eastern Pyrenees, U-Pb zircon geochronology, rheomorphic ignimbrites

1

New Late Middle to Early Upper Ordovician U-Pb zircon ages of extension-related felsic volcanics in the Eastern Pyrenees (NE Iberia): Tectonic implications.

Joan Martí[1], Luigi Solari[2], Josep Maria Casas[3], Martim Chichorro[4]

1. Group of Volcanology. Institute of Earth Sciences Jaume Almera, CSIC, Lluís Solé Sabarís s/n, 08028 Barcelona, Spain.
2. Centro de Geociencias, UNAM, Campus Juriquilla, 76230 Queretaro, Mexico.
3. Departament de Dinàmica de la Terra i de l'Oceà-Institut de Recerca Geomodels, Facultat de Ciències de la Terra, Universitat de Barcelona, Martí i Franquès s/n, 08028 Spain.
4. GEOBIOTEC, Departamento de Ciências da Terra, Universidade Nova de Lisboa, Portugal

Abstract

Pre-Variscan basement rocks from the Pyrenees provide evidence of several magmatic episodes with complex geodynamic histories from the upper Neoproterozoic to the Palaeozoic. One of the most significant episodes, consisting of several granitic and granodioritic bodies and volcanic rocks, mostly pyroclastic in nature, dates from the Upper Ordovician. In the eastern Pyrenees this magmatism is well represented in the Ribes de Freser and Núria areas; here, the Núria orthogneiss and the Ribes granophyre, both dated at ca. 457–460 Ma, seem to form a calc-alkaline plutonic suite emplaced at different crustal levels. The presence of numerous pyroclastic deposits and lavas interbedded with Upper Ordovician (Sandbian-Early Katian, formerly Caradoc) sediments, intruded by the Ribes granophyre, suggests that this magmatic episode also generated significant volcanism. Moreover, the area hosts an important volume of rhyolitic ignimbrites and andesitic lavas affected by Alpine deformation. These volcanic rocks were previously attributed to Late-Variscan volcanism, extensively represented in other areas of the Pyrenees. Here we present the first five laser ablation U-Pb zircon dates for this ignimbritic succession and two new ages of the Ribes granophyre. The ages of the ignimbrites overlapping within error are 460 Ma, the same, suggesting a genetic relation between the plutonic and volcanic rocks and indicating that the Sandbian-Katian magmatism is much

more voluminous than reported in previous studies, and possibly includes mega-eruptions linked to the formation of collapse calderas..

Keywords: Upper Ordovician volcanism, Eastern Pyrenees, U-Pb zircon geochronology, rheomorphic ignimbrites

Introduction

The Pyrenees are a WNW-ESE trending Alpine fold and thrust belt that contains pre-Variscan basement rocks, late Neoproterozoic-to-Carboniferous in age. Pre-Variscan basement rocks form a large belt in the core of the cordillera and provide evidence of several pre-Variscan and Variscan magmatic episodes. Recently, the extensive use of U-Pb zircon geochronology, together with new geochemical and isotopic data, have produced significant advances in the understanding of these magmatic episodes, including the importance of subduction-related Ediacaran magmatism (Castiñeiras et al. 2008; Casas et al. 2015; Padel et al., 2017), Ordovician magmatic events linked to the formation of the northern Gondwana passive margin (Cocherie et al. 2005; Castiñeiras et al. 2008; Casas et al. 2010; Navidad et al. 2010) and Carboniferous magmatic rocks formed during the Variscan collision (Pereira et al. 2014; Denèle et al. 2014; Martínez et al. 2016; Van Lichtervelde et al. 2017). In some cases, where there is a lack of fossils and of reference stratigraphic horizons, the geochronological data also enable us to assess the age of the pre-Middle Paleozoic metasedimentary sequences and correlate them along the whole margin (Padel et al. 2017). This is the case for the pre-Upper Ordovician sequences of the eastern Pyrenees where Ediacaran, Ordovician and Carboniferous magmatic rocks are interbedded with or mainly intrude into an almost unfossiliferous thick (up to 5000? m) pre- Upper Ordovician series.

In this study we focus on a thick sequence of strongly welded, rheomorphic (i.e: showing secondary flow structures) rhyolitic ignimbrites that crop out extensively in the Campelles-Bruguera area, along the southern slope of the Canigó massif, (Fig. 1). These volcanic rocks were initially attributed to Upper Carboniferous-Lower Permian magmatism (Robert, 1980), lying unconformably

on an undated pre-Variscan slate-dominated succession (Cambrian-Ordovician?; Muñoz, 1985). We present new geochronological results that demonstrate these rocks correspond to a late Middle to early Upper Ordovician magmatic event rather than a late Palaeozoic one. Unlike other Unlike other Ordovician igneous rocks in the Pyrenees, the impressive volume of the rhyolitic ignimbrites represent an important volcanic event. We compare our new radiometric ages with existing ones from plutonic and subvolcanic rocks from the same late Middle to early Upper Ordovician magmatic episode found near the study area and suggest a possible genetic relationship among all of them..

Geological setting

Ordovician magmatic events have been well studied in most of the Ordovician terrains of the North Gondwana margin and other margins of the Rheic Ocean (Holland and Patzkowsky, 1996; Herrmann et al., 2004; Finney and Berry, 2010, and references herein; Huff et al., 2010), where they are mainly represented by calc-alkaline granites and granodiorites, and silicic volcanic rocks. A number of large eruptions that may even had implications for climate change have also been identified from the period (Huff et al., 1992; Young et al. 2009; Buggisch et al., 2010; Hermann et al., 2010; Lefebvre et al., 2010; Sell et al., 2013; Jones et al., 2017). In Alpine peri-Mediterranean domains, Ordovician magmatic rocks are well represented in several areas, including the French Massif Central (Roger et al., 2004; Pitra et al., 2012; Lotout et al. 2017), Sardinia (Helbing and Tiepolo, 2005; Gaggero et al., 2012), Sicily (Trombetta et al., 2004) and the central, southern and eastern Alps (Heinisch, 1981; Zurbriggen et al., 1997; von Raumer, 1998; Guillot et al., 2002; Schaltegger et al., 2003).

In the Pyrenees, Ordovician magmatic events form part of successive magmatic pulses that are well documented in the pre-Variscan basement rocks (Figs. 1 and 2). According to radiometric data, this Ordovician magmatism lasted for about 30 myr (ca. 477–446 Ma) (Castiñeiras et al., 2008; Denéle et al., 2009; Casas et al., 2010; Martinez et al., 2011; Mezger and Gerdes, 2016) and although the magmatic activity seems to be continuous, geochronological and geochemical data reveal the

existence of two separate magmatic events, one of Lower to Middle Ordovician age and the other of late Middle to Upper Ordovician age. The Lower-Middle Ordovician magmatic events (ca. 477-467 Ma) gave rise to voluminous granites that constitute the protoliths of the gneisses of the Aston, Hospitalet, Canigó, Roc de Frausa and Albera massifs (Cocherie et al. 2005; Castiñeiras et al. 2008; Denèle et al. 2009; Liesa et al. 2011; Mezger and Gerdes 2016). Lower-Middle Ordovician granites are of calc-alkaline and metaluminous composition and some authors relate to arc magmatism, generated by subduction beneath the northern Gondwanan margin (e.g., von Raumer et al., 2003; von Raumer and Stampfli, 2008). It should be noted that coeval mafic plutonic and silicic volcanic rocks are scarce. By contrast, the late Middle to Upper Ordovician magmatic pulse (ca. 467-446 Ma) yielded a varied suite of magmatic rocks especially well represented in the Canigó massif: calc-alkaline ignimbrites, andesites, volcaniclastic rocks, diorites and various types of small granitic bodies (Martí et al., 1986; Casas et al., 2010; Martinez et al., 2011).

The Ediacaran-Lower Ordovician sedimentary sequence, that crops out extensively in the Central and Eastern Pyrenees, is covered unconformably by a well dated Upper Ordovician succession (Cavet, 1957; Hartevelt, 1970). This younger succession constitutes a broad, fining-upward megasequence of clastic deposits bearing a key limestone-marlstone interbed, which lies unconformably upon older Cambrian-Ordovician beds (Santanach 1972; García-Sansegundo et al., 2004; Casas and Fernández 2007; Padel et al., in press) (Figs. 2, 3 and 4), and which has been interpreted as related to extensional tectonics (e.g., García-Sansegundo et al., 2004; Alvaro et al., 2018; Puddu et al., 2018). The presence of volcanic rocks interbedded with the Upper Ordovician sediments has been noted from Pierrefite (Calvet et al., 1988) and but mainly from the Ribes de Freser area (Robert and Thiebaut, 1976; Robert, 1980; Ayora, 1980). These volcanic rocks compose a predominantly pyroclastic succession, which indicates the predominantly explosive character of this volcanic episode; associated lavas and subvolcanic intrusive rocks are scarce (Martí et al. 1986). The composition of these pyroclastic rocks includes andesite, rhyodacite and rhyolite and in volume

provide only a relatively minor contribution to the sedimentation of their corresponding Ordovician basins.

Additionally, our study area (Campelles-Bruguera, along southern slope of the Canigó) includes a subvolcanic granitic body, the Ribes granophyre, an undeformed, fine-grained, leucocratic granofels with a microscopic granophyric texture, emplaced in the lower part of the Sandbian-Early Katian succession and dated at 458±3 Ma by Martinez et al. (2011) (Figs. 2, 3 and 4 a-d). Several other granitic orthogneissic bodies are emplaced in the lower part of the pre-Variscan succession: for example, the Núria gneiss is a homogeneous, medium-to-coarse-grained, two-mica granite gneiss (protolith age of 457±4 Ma, Martinez et al 2011), and the contemporaneous Queralbs gneiss is an augen gneiss that forms a ring around and on top of this two-mica gneiss (with a igneous crystallization age of 457±5 Ma, Martínez et al., 2011, who used the name Núria augen gneis for the Queralbs gneiss).

In addition to volcanic rocks clearly interbedded with Upper Ordovician sediments, the study area contains a thick (> 1000 m) succession of rheomorphic rhyolitic ignimbrites (the Campelles-Bruguera ignimbrites), occasionally associated at their bases with basaltic andesites (Figs. 2, 3 and 4 e-f). This succession lies unconformably over undated rocks, attributed to the Cambrian or early Ordovician (Muñoz, 1985), that include an occasional thin, poorly exposed succession of continental sedimentary fan deposits. The presence of some pollen remains in these fan deposits motivated Robert (1980) to attribute them and the overlaying volcanic rocks to a Late Paleozoic volcanic episode whose effects are noted throughout the Pyrenees. This assumption was never questioned by subsequent studies (Muñoz, 1986; Martí, 1986; 1991) despite the fact that these pollen remains were described as "badly preserved and poor representative association that is insufficient to precisely indicate the age of the sediment" by Robert (1980). The ignimbrites are rhyolitic in composition and show clear secondary silicification due to post-emplacement alteration processes (Martí, 1986). They are very crystal-poor possessing only phenocrysts of sodium-rich plagioclase, quartz and minor biotite. The main characteristic of these rocks is their flow banding with some flow folds caused by the extreme

stretching and welding of the original pumice fragments due to rheomorphism (Martí, 1986) (Fig. 4 e-f). Stretched pumices (fiammes) are still visible in some outcrops, evidence of their primary pyroclastic character (Fig. 4f).

In the Pyrenees Lower-Middle Ordovician magmatic events developed during an episode of folding, uplift and erosion that led to the formation of the Upper Ordovician ("Sardic") unconformity, whereas a subsequent extensional pulse developed normal faults that controlled the post-Sardic sediments and infilled palaeorelief depressions (García-Sansegundo et al., 2004; Casas and Fernández, 2007; Casas, 2010). In order to complete our understanding of the Middle-Upper Ordovician magmatism, we present here the first zircon U-Pb age data from the thick sequence of rheomorphic rhyolitic ignimbrites outcropping in the vicinity of the towns of Campelles and Bruguera. This succession of volcanic rocks was deformed during the Variscan orogeny but is not affected by metamorphism. It is only partially affected by post-emplacement hydrothermal alteration that produced the silicification of the original glass components and transformed the juvenile phenocrysts into clay aggregates, microcrystalline quartz and carbonates, but their original forms and textures are preserved.

Analytical Methodology

To determine the age of the Campelles-Bruguera welded ignimbrites, we selected five samples (CAM-6, CAM-7, CAM-9, CAM-13 and CAM-18) that were prepared for laser ablation inductively coupled plasma mass spectrometry (LA-ICP-MS) isotopic dating of single zircon crystals. Samples CAM 18, CAM 6 and CAM 7 are located, from base to top, respectively, along the same rheomorphic ignimbrite unit, cropping out about 4 km west of the town of Campelles (Fig. 2). Sample CAM 9 corresponds to the same unit that occurs in an isolated outcrop about 2 km north of Campelles. Sample CAM 13 comes from a thick unit of rheomorphic ignimbrites located north of the town of Brugera (Fig. 2). We also collected two samples (CAM-11 and CAM-12) from the Ribes granophyre that was previously dated by Martinez et al. (2011). Zircon grains were separated from fresh rock samples in the FCT-UNL laboratories using standard heavy mineral separation techniques

including the application of heavy liquids and a Frantz isodynamic separator. The final selection of the zircon grains for U-Pb dating was performed by hand-picking under a binocular microscope. Most euhedral zircons, with well-preserved facets and no sign of resorption were selected for analysis. Prior to analysis, the mounted and polished grains were imaged under cathodoluminescence, using an ELM-3R luminoscope (Marshall et al., 1988). CL images were used to avoid inclusions of minerals that can contain radiogenic Pb (e.g. apatite), and to avoid analysing inherited cores and overgrowths.

The laser ablation system at Laboratorio de Estudios Isotópicos, Centro de Geociencias, UNAM, has been described by Solari et al. (2010). It consists of a Thermo ICap Qc quadrupole ICPMS equipped with an LPX 200 Excimer laser, and a new M151 two-volume cell,

with even greater stability than the cell described by Müller et al. (2009). The instrument is run through a Resonetics M050 workstation. A 'squid' signal homogeniser is used immediately after the cell, approximately 2 m before the ablated material enters the plasma. A total of 350 ml of He is used as carrier gas and mixed downstream with 4.5 ml of N2. A frequency of 5 Hz was used during the work, with a constant on-target fluence of 6 J/cm^2, measured with an external energy meter. An analytical spot of 23 μm was systematically used throughout the whole study, while the pit depth is estimated to be less than 8 μm . The zircon standard 91500 (Wiedenbeck et al. 2004) was used as the primary standard, and the Plešovice standard (Slama et al., 2008) was employed as secondary (quality control) standard. Both were interspersed in the sequence with unknown zircon crystals: two 910500 and one Plešovice followed by 10 unknown zircon grains, Additionally, NIST SRM 610 was also analyzed to calculate the elemental concentrations in zircon, monitored to check for inclusions or subtle changes in composition that could be indicative of different domains. We used ^{29}Si as an internal standard, assuming a stoichiometry of 32.77% SiO_2 in zircon.

The data reduction was performed using Iolite 3.0 (Paton et al., 2010; 2011) employing the VizualAge data reduction scheme developed by Petrus and Kamber (2012). Uncertainties of the primary standard during the analytical session were propagated using Iolite protocols. The calculated age uncertainties correspond to 2 standard errors. Data were exported from Iolite and the concordia diagrams and weighed mean dates were calculated and plotted using Isoplot v.3.7 (Ludwig, 2008). No common Pb correction was applied as the small ^{204}Pb count rates were insignificant when compared to the ^{204}Hg signal typically seen in our system. Analyses that fell outside +30% and -5% discordancy, or which had more than 10% 2-sigma errors, were discarded. The external reproducibility of the Plešovice secondary standard measured during the analytical session in which the current analyses were performed yielded a mean ^{206}Pb/^{238}U age of 3 340.7 ± 1 Ma (2SE, n=39, MSWD= 1.1). The range of this variation is -0.86 to +0.71% of the (recalculated) accepted ^{206}Pb/^{238}U date of Horstwood et al (2016) that corresponds to 337.16±0.11 Ma. The long-term variation of the secondary standard is thus within the accepted uncertainty for the LA-ICPMS dating, currently stated at ca. 1-2% (e.g. Klotzli et al, 2009; Horstwood et al., 2016)

Results

The seven selected samples described above yielded 218 U-Pb analyses that, after filtering, were used to determine crystallization ages. Oscillatory zoning, observed under cathodoluminescence, was interpreted as magmatic. The analyses performed on those domains were thus interpreted as indicative of zircon crystallization in the magma chamber" Results are presented in Figure 5 (and Table 1, supplementary material).

Thirty zircon crystals were analyzed from the ignimbrite sample CAM-6, collected from the middle zone of the thick ignimbritic succession of Campelles (Fig. 2). In all, 24 satisfied the filtering criteria. Some of the zircon crystals are prismatic and stubby in shape, barely zoned under CL, and cluster around a mean ^{206}Pb/^{238}U date of 459.5±4.2 Ma (n=12, MSWD= 1.4), which is interpreted as the crystallization age of the ignimbrite Some other crystals with anhedral to corroded shapes yielded

older ages, ranging from the Neoproterozoic (the youngest, 824 Ma) to the Paleoproterozoic and even Neoarchean (Fig. 5A). One slightly discordant younger crystal is indicative of Pb loss.

Sample CAM-7 corresponds to top of the same ignimbrite unit as sample CAM-6. Only 20 zircon crystals were recovered, 17 of which met the filtering criteria. They are up to 280 μm in length, generally prismatic and elongated. Under CL they show oscillatory zoning developed parallel to the crystallographic c-axis. A group of 10 analyses straddle the concordia curve, with a mean $^{206}Pb/^{238}U$ age of 459.1± 5.3 Ma (N= 10, MSWD= 2.1), interpreted as the ignimbrite crystallization age (Fig. 5B). A few zircons grains were younger and variably discordant, indicative of Pb loss, whereas three others were older inherited crystals ranging from 652 to ca. 2300 Ma in age.

CAM-18 belongs to the base of the same welded ignimbrite unit as samples CAM-7 and CAM-6. Out of the 35 analyzed zircon crystals, 33 met the filtering criteria. They range from elongated prisms with pyramidal terminations, to short and stubby. Under CL they show moderate luminescence, with faint oscillatory zoning. Most analyses are concordant including six grains that give older ages (Neoproterozoic, Ediacaran to Cryogenian in age, Table 1), which we interpret as xenocrysts (Fig. 5C). The most abundant group clusters on the Concordia curve and gives a mean $^{206}Pb/^{238}U$ date of 460.4±2.2 Ma (21 analyses, MSWD= 0.96, Fig. 5C) which we interpret as the age of ignimbrite crystallization.

Sample CAM-9 also consists of a welded ignimbrite cropping out several kilometers towards the NW from the site of samples CAM-6, CAM-7, and CAM-18. Only 20 zircon grains were recovered from CAM-9, 16 of which satisfied the filtering criteria. They are small compared with zircons from the previously described samples, not exceeding 140 μm, with mostly oval to rounded morphologies. Although being poorly luminescent under CL, igneous zoning is observable in some of the crystals. Few of these crystals are concordant, instead most are variably discordant (Fig. 5D). Three of the least discordant are Ediacaran, ranging in age from 592 to 625 Ma (Table 1); the others range in age from the early Neoproterozoic to the Paleoproterozoic. While stratigraphic correlations

suggest for this unit a similar Ordovician age as the other dated samples, we were unable to recover any magmatic zircon..

Sample CAM-13 corresponds to a different outcrop of welded ignimbrite, belonging to the Bruguera succession (Fig. 2). In all, 33 out of 35 analyzed zircon crystals met the filtering criteria. They are stubby grains with bipyramidal terminations, faintly zoned under CL and up to 220 μm in length. Most of the analyzed crystals are concordant. Apart from one clearly inherited zircon, with an apparent age of 759±28 Ma, and another, slightly discordant one with an apparent age of 379±12 Ma, almost all the other crystals define a cluster whose mean $^{206}Pb/^{238}U$ age of 459.6±1.9 Ma (N=26, MSWD= 0.46) is interpreted as the age of crystallization (Fig. 5E).

Finally, samples CAM-11 and CAM-12 both belong to a granophyre, previously dated at 458±3 Ma by Martínez et al. (2011). In all, 35 zircon grains were analyzed from sample CAM-11, all of which except one met the filtering criteria. They range in shape from elongated to bipyramidal short prisms, up to 260 μm in length. Under CL, they show homogeneous luminescence, with faint oscillatory-zoning only developed in few crystals. A few of the analyzed zircon grains were slightly discordant. A group of 23 coherent analysis yield a mean $^{206}Pb/^{238}U$ date of 460.1±2 Ma (N= 23, MSWD=0.49), interpreted as the age of granophyre crystallization (Fig. 5F, inset). A small number of zircon crystals, although concordant, yield a slightly older mean age of ca. 488 Ma, and probably correspond to either inherited grains or antecrysts formed in the magma chamber during an earlier episode of magma crystallization. Three discordant grains ranging from ca. 438 to ca. 410 Ma are interpreted as recording Pb loss. Sample CAM-12 also yielded a good number of zircon crystals, 35 of which were analyzed and met the filtering criteria. They are generally stubby and bipyramidal, up to 240 μm in length, although some are fragmented prisms belonging to larger crystals. Under CL they often show oscillatory zoning, with some high-luminescent inclusions, possibly apatite crystals. Apart from a few discordant data, which probably experienced Pb loss, the overall behavior of the remaining crystals have a consistent age. The mean $^{206}Pb/^{238}U$ date of 461.5±2.3 Ma (N= 25, MSWD= 1.4, Fig. 5G inset) obtained from a coherent group of 25 analyses is interpreted as the crystallization

age of the granophyre. Only two grains were slightly older but discordant; three other younger and discordant analyses probably experienced variable amount of Pb loss.

Discussion and conclusions

The new isotopic ages obtained in this study demonstrate that the Campelles-Bruguera rheomorphic rhyolite ignimbrites, previously attributed to a Late Paleozoic volcanic event, are in fact Sandbian-Katian in age and are part of a Middle-Upper Ordovician magmatic event in the Eastern Pyrenees. In addition to the stratigraphic implications that these results have for understanding the pre-Variscan evolution of Pyrenees, there are also significant implications for the origin, characteristics and importance of volcanism associated with Middle to Late Ordovician magmatism in the Eastern Pyrenees. All the ages obtained indicate that a single magmatic event produced the emplacement of the silicic intrusive Ribes granophyre and Campelles-Bruguera ignimbrites. Despite the fact that volcanic rocks interbedded with Middle-Upper Ordovician metasediments are abundant and present in nearly the whole Middle-Upper Ordovician stratigraphic succession in the Eastern and Central Pyrenees, they were previously recognised as neither volumetrically significant nor indicative of the provenance or location of source vents. The predominance of pyroclastic rocks (e.g. ignimbrites and ashfall beds) was already noted by Martí et al. (1986) as indicative of the explosive character of this volcanism. The recognition of the Campelles-Bruguera rheomorphic ignimbrites as products of the Middle-Upper Ordovician magmatism in this area increases their extent by several thousands of km^3, thereby suggesting that this volcanic episode was much more significant than once thought. This, together with the thickness of the Campelles ignimbritic succession, which is on the order of 1000 m, suggest the occurrence of Sandbian-Katian mega-eruptions possibly linked to the formation of collapse calderas.

First, this implies that much greater magma production was needed to sustain the volcanism and, secondly, that the mechanisms for storing and expelling such large amounts of rhyolitic magmas were favored by the regional and local tectonics operating at that time. Such a large volume of volcanic rocks and their particular characteristics (i.e. rheomorphic ignimbrites) suggest that one or

more large caldera structures were the source of the volcanism in this area, as was suggested when these rocks were still considered to be Late Paleozoic in age (Robert, 1980; Martí, 1986, 1991). Moreover, it has been proposed (Navidad et al 2010) that the most probable tectonic setting for the emplacement of the Middle-Upper Ordovician volcanic and plutonic rocks is an extensional regime.. An extensional geodynamic setting would favour the large-scale eruption of silicic magma, as it occurs in other similar settings in more modern analogs (Basin and Range, USA, Lipman, 1992; Sierra Madre Occidental, México, Aguirre-Díaz and McDowell, 1993). Thus by 460 Ma, the extensional breakup of the Gondwanan margin and the rifting away of terranes, including the Eastern Pyrenees, was in progress.

Existing petrological and geochemical data of the volcanic rocks dated here (Martí, 1986; Martí et al., 1986) reveal a calc-alkaline character coincident with that of the coeval intrusive rocks cropping out in the same area (Martínez et al., 2011). Martínez et al. (2011) proposed that these intrusive rocks were derived from the melting of Ediacaran sediments formed from the erosion of previous Neoproterozoic arc rocks, which were contaminated by older components, possibly due to the partial melting of a pre-Neoproterozoic basement. Inherited Neoproterozoic – and even a few Paleoproterozoic-to-Archean – zircon grains found in nearly all the samples we dated (Fig. 6) support the existence of pre-Neoproterozoic components in the source region of these magmatic rocks. However, pre-Paleozoic crystalline basement does not outcrop in the eastern Pyrenean part of the Variscan Chain and so the exact source of the late Middle-early Upper Ordovician magmas remains uncertain.

The Middle-Upper Ordovician magmatic episode in the Eastern Pyrenees would have been triggered by extensional tectonics affecting a crust previously thickened by a compressional episode of mid-Ordovician age (Casas, 2010; Navidad et al, 2010), which followed the Neoproterozoic-early Cambrian subduction-related magmatism (Casas et al., 2015). This tectonic scenario involving compression followed by extension resembles the events that occurred at the end of the Variscan orogeny in relation to the Upper Carboniferous-Lower Permian volcanism, which is widely found

throughout the Pyrenees in pull-apart basins. These basins were generated during a late-orogenic extensional phase that also generated large-volume eruptions of calc-alkaline magmas (Gisbert, 1981; Martí, 1986; Gilbert, 1989; Lago et al., 2004). This Late-Paleozoic volcanism was coeval with the emplacement of granodioritic plutons at very shallow crustal levels (García-Sansegundo et al., 2004; Pereira et al., 2013). Likewise, our new age data show that all studied magmatic products from the area attributed to a Middle-Upper Ordovician magmatic episode – i.e. the Núria gneisses, the Ribes granophyre and the Campelles-Bruguera volcanic rocks – lie within a very narrow age range. Consequently, we must assume that all these magmatic products have a genetic connection. However, the lack of xenocrysts in the Ribes granophyre, in contrast with their presence in most of the ignimbritic samples, poses an interesting question on whether or not both magmas shared the same source, which deserves to be investigated in further studies in order to understand this potential plutonic-volcanic connection.

Acknowledgments

Financial support for this work was provided by the projects CGL2015-66335-C2-1-R, CGL2017-87631-P, and CGL2017-84901-C2-1-P from Spanish MINECO. JM is grateful for the MECD (PRX16/00056) grant. We would like to thanks Carlos Ortega-Obregón (CGEO, UNAM) for the instrument maintenance and U-Pb determinations. We thank the Editor, C. Dietsch, and an anonymous referee for their constructive reviews. English text was reviewed and corrected by Michael Lockwood.

References

Aguirre-Díaz, G.J., McDowell, F.W., 1993. Nature and timing of faulting and synextensional magmatism in the southern Basin and Range, central-eastern Durango, México: Geological Society of America Bulletin, 105, 1435–1444.

Alvaro, J. J., Casas, J. M., Clausen, S., Quesada, C., 2018. Early Palaeozoic geodynamics in NW Gondwana. Journal of Iberian Geology, 44:551–565 https://doi.org/10.1007/s41513-018-0079-x

Ayora, C., 1980. Les concentracions métal.liques de la Vall de ribes. PhD Thesis, Univ. Barcelona, 236 pp.

Buggisch. W., Joachimski, M. M., Lehnert, O., Bergstrom, S. M., Repetski, J. E., Webers, G. F., 2010. Did intense volcanism trigger the fi rst Late Ordovician icehouse?. Geology, 38, 327–330; doi: 10.1130/G30577.1

Calvet, P., Lapierre, H., Charvet, J. 1988. Diversité du volcanisme Ordovicien dans la région de Pierrefitte (Hautes Pyrénées): rhyolites calco-alcalines et basaltes alcalins. Comptes Rendus de l'Académie des Sciences de Paris, D 307, 805-812.

Casas, J.M. 2010. Ordovician deformations in the Pyrenees: new insights into the significance of pre-Variscan ('sardic') tectonics. Geological Magazine, 147, 674–689.

Casas, J.M., Fernández, O., 2007. On the Upper Ordovician unconformity in the Pyrenees: New evidence from the La Cerdanya area. Geologica Acta 5, 193–198.

Casas, J.M., Castiñeiras, P., Navidad, M., Liesa, M. and Carreras, J. 2010. New insights into the Late Ordovician magmatism in the Eastern Pyrenees: U–Pb SHRIMP zircon data from the Canigó massif. Gondwana Research, 17, 317-324.

Casas, J. M., Navidad, M., Castiñeiras, P., Liesa, M., Aguilar, C., Carreras, J., Hofman, M., Gärtner, A., Linnemann, U., 2015. The Late Neoproterozoic magmatism in the Ediacaran series of the Eastern Pyrenees: new ages and isotope geochemistry. International Journal of Earth Sciences 104, 909–925.

Castiñeiras, P., Navidad, M., Liesa, M., Carreras, J. and Casas, J.M. 2008. U-Pb zircon ages (SHRIMP) for Cadomian and Lower Ordovician magmatism in the Eastern Pyrenees: new insights in the pre-Variscan evolution of the northern Gondwana margin. Tectonophysics, 461, 228-239.

Cavet, P., 1957. Le Paléozoïque de la zone axiale des Pyrénées orientales françaises entre le Roussillon et l'Andorre. Bulletin Service Carte Géologique France 55, 303–518.

Cocherie, A., Baudin, Th., Autran, A., Guerrot, C., Fanning, C..M, Laumonier, B., 2005. U-Pb zircon (ID-TIMS and SHRIMP) evidence for the early Ordovician intrusion of metagranites in the late Proterozoic Canaveilles Group of the Pyrenees and the Montagne Noire (France). Bull Soc géol Fr 176:269–282.

Cohen, K.M., Finney, S.C., Gibbard, P.L., Fan, J.-X., 2013 (updated) The ICS International Chronostratigraphic Chart. Episodes 36: 199-204.

Deloule, E., Alexandrov, P., Cheilletz, A., Laumonier, B., Barbey, P. (2002) In-situ U-Pb zircon ages for Early Ordovician magmatism in the eastern Pyrenees, France: the Canigou orthogneisses. Int. J. Earth Sci., 91, 398–405.

Denèle, Y., Barbey, P., Deloule, E., Pelleter, E., Olivier, P., Gleizes, G., 2009. Middle Ordovician U–Pb age of the Aston and Hospitalet orthogneissic laccoliths: their role in the Variscan evolution of the Pyrenees. Bull. Soc. Geol. Fr. 180, 209–216.

Denèle, Y., Laumonier, B., Paquette, J.L., Olivier, P., Gleizes, G., Barbey, P. 2014. Timing of granite emplacement, crustal flow and gneiss dome formation in the Variscan segment of the Pyrenees. In: Schulmann, K., Martínez Catalán, J.R., Lardeaux, J.M., Janousek, V. & Oggiano, G. (eds). The Variscan Orogeny: Extent, Timescale and the Formation of the European Crust. Geological Society, London, Special Publications, 405, 265–287. http://dx.doi.org/10.1144/SP405.5

Finney, S. C., Berry, W. B. N (eds) 2010. The Ordovician Earth System. The Geological Society of America, Special Paper, 466, 193 pp.

Gaggero, L., Oggiano, G., Funedda, A., Buzzi, L. 2012. Rifting and Arc-Related Early Paleozoic Volcanism along the North Gondwana Margin: Geochemical and Geological Evidence from Sardinia (Italy). The Journal of Geology, 120, 273–292

García- Arias, M., Corretgé, L. G., Castro, A., 2012. Trace element behavior during partial melting of Iberian orthogneisses: An experimental study. Chemical Geology, 292–293, 1-17

García-Sansegundo, J., Gavaldà, J., Alonso, J. L., 2004. Preuves de la discordance de l'Ordovicien supérieur dans la Zone Axiale des Pyrénées: exemple du Dôme de la Garonne (Espagne, France). Comptes Rendus Geosciences, 336, 1035–1040.

García-Sansegundo, J., Poblet, J., Alonso, J. L., Clariana, P., 2011. Hinterland-foreland zonation of the Variscan orogen in the Central Pyrenees: comparison with the northern part of the Iberian Variscan Massif. In From: Poblet, J. and Lisle, R. J. (eds) Kinematic Evolution and Structural Styles of Fold-and-Thrust Belts. Geological Society, London, Special Publications, 349, 169–184. DOI: 10.1144/SP349.9

Gilbert, J.S., 1989. The Late-Hercynian volcanism of the Pyrenees. PhD Thesis, University of Cambridge (unpubl.).

Gisbert, J. (1981): Estudio geológico-petrológico del Estefaniense-Pérmico de la Sierra del Cadí (Pirineos de Lérida). Diagénesis y sedimentologia. Tesi de Doctorat, Univ. de Zaragoza: 313 pp.

Gradstein, F.M., Ogg, J.G., Smith, A.G., 2004. A Geologic Time Scale 2004. Cambridge University Press, Cambridge

Guillot, F., Schaltegger, U., Bertrand, J.M., Deloule, E., Baudin, T., 2002. Zircon U–Pb geochronology of Ordovician magmatism in the polycyclic Ruitor Massif (Internal W-Alps). International Journal of Earth Sciences 91, 964–978.

Guitard, G., Autran, A, Fonteilles, M, 1996. Le substratum precambrien du Paleozolque, In: Barnolas,A, Chiron,J,C (Eds,), Synthese geologique etgeophisique des Pyrenees, VOL 1. BRGM-ITGE, Orleans, pp, 137-156,

Handy, M.R., Franz, L., Heller, F., Janott, B., Zurbriggen, R., 1999. Multistage accretion and exhumation of the continental crust (Ivrea crustal section, Italy and Switzerland). Tectonics 18, 1154–1177.

Hartevelt, J. J. A. 1970. Geology of the Upper Segre and Valira valleys, Central Pyrenees, Andorra/Spain. Leidse Geologische Mededelingen, 45, 167–236.

Heinisch, H., 1981. Preliminary report on Early Paleozoic acidic volcanism in the Eastern and Southern Alps — a review. In: Karamata, S., Sassi, F.P. (Eds.), IGCP no 5: Newsletter, vol. 3, pp. 80–88.

Helbing, H., Tiepolo, M., 2005. Age determination of Ordovician magmatism in NE Sardinia and its bearing on Variscan basement evolution. Journal Geological Society London 162, 689–700

Herrmann,A. D., Macleod, K. G., Leslie, S. A., 2010. 3Did a volcanic mega-eruption cause global cooling during the Late Ordovician? PALAIOS, 25, 831–836

Herrmann, A.D., Haupt, B.J., Patzkowsky, M.E., Seidov, D., Slingerland, R.L., 2004, Response of Late Ordovician paleoceanography to changes in sea level, continental drift, and atmospheric pCO2: Potential causes for long-term cooling and glaciation: Palaeogeography, Palaeoclimatology, Palaeoecology, 210, 385–410.

Holland, S.M., Patzkowsky, M.E., 1996, Sequence stratigraphy and long-term paleoceanographic change in the Middle and Upper Ordovician of the eastern United States, in Witzke, B.J., Ludvigson, G.A., Day, J., Paleozoic Sequence Stratigraphy; Views from the North American Craton: Geological Society of America Special Paper, v. 306, p. 117–129.

Horstwood, M. S. A., Košler, J., Gehrels, G., Jackson, S. E., McLean, N. M., Paton, C., et al., 2016. Community-Derived Standards for LA-ICP-MS U-Th-Pb Geochronology – Uncertainty Propagation, Age Interpretation and Data Reporting. Geostandards and Geoanalytical Research. http://doi.org/10.1111/j.1751-908X.2016.00379.x

Huff, W. D., Bergstrom, S. M., Kolata, D. R., 1992. Gigantic Ordovician volcanic ash fall in North America and Europe: biological, tectonomagmatic, and event-stratigraphic significance. Geology, 20, 875-878.

Huff, W. D., Bergstrom, S. M., Kolata, D. R., 2010. Ordovician Explosive volcanism. In Finney, S. C., Berry, W. B. N (eds) 2010. The Ordovician Earth System. The Geological Society of America, Special Paper, 466, 193 pp.

Jones, D. S., Martini, A. M., Fike, D. A., Kaiho, K., 2017. A volcanic trigger for Late Ordovician mass extinction?. Mercury data from south China and Laurentia. Geology, DOI: 10.1130/G38940.1

Klötzli, U., Klötzli, E., Günes, Z., Kosler, J. 2009. Accuracy of Laser Ablation U-Pb Zircon Dating: Results from a Test Using Five Different Reference Zircons. Geostandards and Geoanalytical Research, 33, 5-15. https://doi.org/10.1111/j.1751-908X.2009.00921.x

Lago, M., Arranz, E., Pocovi, A., Gale, C., Gil-Imaz, A. 2004. Permian magmatism and basin dynamics in the southern Pyrenees: a record of the transition from late Variscan transtension to early Alpine extension. In: Wilson, M., Neumann, E.-R., Davies, G.R., Timmerman, M.J., Heeremans,M., Larsen, B.T. (Eds.), Permo-Carboniferous Magmatism and Rifting in Europe: Geological Society, London, Special Publications, 223, p. 439464.

Lefebvre, V., Servais, T., François, L., Averbuch, O. 2010. Did a Katian large igneous province trigger the Late Ordovician glaciation?. Paleogeography, Paleoclimatology, Paleoecology. 296 (3), 310-319.

Lotout, C., Pitra, P., Poujol, M., Van Den Driessche, J. (2017). Ordovician magmatism in the Lévézou massif (French Massif Central): tectonic and geodynamic implications. International Journal of Earth Sciences, 106/2, 501–515. DOI : 10.1007/s00531-016-1387-z

Liesa, M., Carreras, J., Castineiras, P., Casas, J.M., Navidad, M., Vila, M., 2011. U–Pb zircon age of Ordovician magmatism in the Albera Massif (Eastern Pyrenees). Geol. Acta 9 (1), 93–101

Lipman, P.W., 1992, Magmatism in the Cordilleran United States: Progress and problems, In Burchfiel, B. C., Lipman, P. W., Zoback, M. L., eds, The Cordilleran Orogen: Conterminous U. S.: Boulder, Colorado, Geological Society of America, The Geology of North America, v. G-3, 481–514.

Ludwig, K., 2008. Manual for Isoplot 3.7: A Geochronological Toolkit for Microsoft Excel Berkeley Geochronology Center, Berkeley, CA, Special Publication No. 4, p. 77 (rev. August 26).Martí,

J., 1986. El volcanisme explosiu tardihercinia del Pirineu Catala. PhD. Thesis, University of Barcelona, (unpubl), 303 pp.

Martí, J., 1991, Caldera-like structures related to Permo-Carboniferous volcanism of the Catalan Pyrenees (NE Spain). J. Volcanol. Geotherm. Res., 45: 173-186.

Martí, J., Muñoz, J.A., Vaquer, R., 1986. Les roches volcaniques de l'Ordovicien supérieur de la région de Ribes de Freser-Rocabruna (Pyrénées catalanes): caractères et signification. Comptes Rendus de l'Académie des Sciences de Paris 302, 1237–1242.

Martínez, F.J., Iriondo, A., Dietsch, C., Aleinikoff, J.N., Peucat, J.J., Cirès, J. Reche, J., Capdevila, R., 2011. U-Pb SHRIMP-RG zircon ages and Nd signature of lower Paleozoic rifting-related magmatism in the Variscan basement of the Eastern Pyrenees. Lithos, 127, 10-23.

Martínez F.J., Dietsch C., Aleiniikoff J., Cirés J., Arboleya M.L., Reche J., Gómez-Gras D., 2016. Provenance, age, and tectonic evolution of Variscan flysch, southeastern France and northeastern Iberia based on zircon geochronology. Geological Society of America Bulletin, 128, 5/6, 842-859. doi: 10.1130/B231316.1.

Mezger, J., Gerdes, A., 2016. Early Variscan (Visean) granites in the core of central Pyrenean gneiss domes: implications from laser ablation U-Pb and Th-Pb studies. Gondwana Res 29:181–198.

Müller, W., Shelley, J.M.G., Miller, P., Broude, S., 2009. Initial performance metrics of a new custom-designed ArF excimer LA-ICP-MS system coupled to a two volume laser-ablation cell. Journal of Analytical Atomic Spectrometry, 24, 209–214. doi: 10.1039/b805995k.

Muñoz, J.A., 1985. Estructura alpina i herciniana a la vora sud de la zona axial del Pirineu Oriental. PhD Thesis, University of Barcelona, (unpubl.).

Muñoz, J. A. 1992. Evolution of a continental collision belt: ECORS-Pyrenees crustal balanced cross-section. In Thrust Trectonics (ed. K. R. Mc Clay), pp. 235–46. London: Chapman & Hall.

Murphy, B.J., Gutiérrez Alonso, G., Fernández Suárez, J., Braid, J., 2008. Probing crustal and mantle lithosphere origin through Ordovician volcanic rocks along the Iberian passive margin of Gondwana. Tectonophysics 461, 166–180.

Navidad, M., Casas, J.M., Castiñeiras, P., Barnolas, A., Fernández-Suárez, J., Liesa, M., Carreras, J., Gil-Peña, I., 2010. Geochemical characterization and isotopic age of the Caradocian magmatism from North-Eastern Iberian Peninsula: Insights from the Late Ordovician evolution of the northern Gondwana margin. Gondwana Research, 17 (2–3), 325–337

Padel, M., Alvaro, J., Casas, J. M., Clausen, S., Poujol, M., Sánchez-García, T., 2017. Cadomian volcanosedimentary complexes across the Ediacaran–Cambrian transition of the Eastern Pyrenees, southwestern Europe. International Journal of Earth Sciences. doi: 10.1007/s00531-017-1559-5

Padel, M., Clausen, S., Alvaro, J., Casas, J.M., in press. Review of the Ediacaran-Lower Ordovician (pre-Sardic) stratigraphic framework of the Eastern Pyrenees, southwestern Europe. Geologica Acta.

Paton, C., Hellstrom, J., Paul, B., Woodhead, J., Hergt, J., 2011. Iolite: Freeware for the visualisation and processing of mass spectrometric data. Journal of Analytical Atomic Spectrometry, 26(12), 2508. http://doi.org/10.1039/c1ja10172b

Paton, C., Woodhead, J. D., Hellstrom, J. C., Hergt, J. M., Greig, A., Maas, R., 2010. Improved laser ablation U-Pb zircon geochronology through robust downhole fractionation correction. Geochemistry Geophysics Geosystems, 11, Q0AA06. http://doi.org/10.1029/2009GC002618

Pereira, J., Castro, A., Chichorro, M., Fernández, C., Díaz-Alvarado, J., Martí, J., Rodríguez, C. (2013). Chronological link between deep-seated processes in magma chambers and eruptions: Permo-Carboniferous magmatism in the core of Pangaea (Southern Pyrenees). Gondwana Research, 25, 290–308

Petrus, J. A., Kamber, B. S., 2012. VizualAge: A Novel Approach to Laser Ablation ICP-MS U-Pb Geochronology Data Reduction. Geostandards and Geoanalytical Research, 36(3), 247–270. http://doi.org/10.1111/j.1751-908X.2012.00158.x

Pitra, P., Poujol, M., Den Driessche, J. V., Poilvet, J.-C., Paquette, J.-L. (2012). Early Permian extensional shearing of an Ordovician granite: The Saint-Eutrope ‘‘C/S-like’’ orthogneiss (Montagne Noire, French Massif Central). C. R. Geoscience, 344: 377–384

Puddu. C., Alvaro, J. J., Casas, J. M., 2018. The Sardic unconformity and the Upper Ordovician successions of the Ribes de Freser area, Eastern Pyrenees. Journal of Iberian Geology (2018) 44:603–617 https://doi.org/10.1007/s41513-018-0084-0

Robert, J.F., 1980. Étude géologique et métallogenétique du val de Ribas sur le versant espagnol del Pyrénées Catalanes. PhD Thesis., Univ. Besançon, 294 pp.

Robert, J.F. and Thiebaut, J. 1976. Découverte d’un volcanisme acide dans le Caradoc de la région de Ribes de Feser (Prov. de Gerone). Comptes Rendus de l’Académie des Sciences de Paris, D 282, 2050-2079.

Roger, F., Respaut, J.P., Brunel, M., Matte, Ph., Paquette, J.L., 2004. Première datation U– Pb des orthogneiss oeillés de la zone axiale de la Montgane Noire (Sud du Massif central): nouveaux témoins du magmatisme ordovicien dans la chaîne varisque. Comptes Rendus Geoscience 336, 19–28.

Santanach, P. F. 1972. Sobre una discordancia en el Paleozoico inferior de los Pirineos orientales. Acta Geológica Hispánica, 7, 129–132.

Sell, B., Ainsaar, L., Leslie, S., 2013. Precise timing of the Late Ordovician (Sandbian) supereruptions and associated environmental, biological, and climatological events. Journal of the Geological Society, London, Vol. 170, 2013, pp. 711–714

Schaltegger, U., Abrecht, J., Corfu, F., 2003. TheOrdovician orogeny in the Alpine basement: constraints from geochronology and geochemistry in the Aar Massif (Central Alps). Schweizerische Mineralogische und Petrologische Mitteilunge 83, 183–195.

Slama, J., Kosler, J., Condon, D., Crowley, J., Gerdes, A., Hanchar, J., et al. (2008). Plešovice zircon — A new natural reference material for U–Pb and Hf isotopic microanalysis. Chemical Geology, 249, 1–35. http://doi.org/10.1016/j.chemgeo.2007.11.005

Solari, L.A., Gómez-Tuena, A., Bernal, J.P., Pérez-Arvizu, O. Tanner, M., 2010. U-Pb zircon geochronology by an integrated LA-ICPMS microanalytical workstation: achievements in precision and accuracy. Geostandards and Geoanalytical Research. DOI: 10.1111/j.1751-908X.2009.00027.x

Trombetta, A., Cirrincione, R., Corfu, F., Mazzoleni, P., Pezzino, A., 2004. Mid-Ordovician U–Pb ages porphyroids in the Peloritan Mountains (NE Sicily): palaeogeographical implications for the evolution of the Alboran microplate. Journal of the Geological Society London 161, 265–276.

Van Lichtervelde, M., Grand'Homme, A., de Saint-Blanquat, M., Olivier, P., Gerdes, A., Paquette, J.-L., Melgarejo, J.C., Druguet, E. and Alfonso, P. , 2017. U-Pb geochronology on zircon and columbite-group minerals of the Cap de Creus pegmatites, NE Spain. Mineralogy and Petrology 111, 1-21.

von Raumer, J.F., 1998. The Paleozoic evolution in the Alps: from Gondwana to Pangea. Geologische Rundschau 87, 407–435.

von Raumer, J.F., Stampfli, G.M., 2008. The birth of the Rheic Ocean — Early Palaeozoic subsidence patterns and subsequent tectonic plate scenarios. Tectonophysics 461, 9–20

von Raumer, J.F., Stampfli, G.M., Bussy, F., 2003. Gondwana-derived microcontinents — the constituents of the Variscan and Alpine collisional orogens. Tectonophysics 365, 7–22.

Wiedenbeck, M., Allé, P., Corfu, F., Griffin, W., Meier, M., Oberli, F., et al. (1995). Three natural zircon standards for U-Th-Pb, Lu-Hf, Trace element and REE Analyses, Geostandard Newsletter, 19(1), 1–23.

Young, S.A., Saltzmann, M.R., Foland, K.A., Linder, J.S., and Kump, L.R., 2009, A major drop in seawater 87Sr/86Sr during the Middle Ordovician (Darriwilian): Links to volcanism and climate?: Geology, v. 37, p. 951–954, doi: 10.1130/G30152A.1.

Zurbriggen, R., Franz, L., Handy, M.R., 1997. Pre-Variscan deformation, metamorphism and magmatism in the Strona-Ceneri Zone (southern Alps of northern Italy and southern Switzerland). Schweizerische Mineralogische und Petrologische Mitteilungen 77, 361–380

List of figures and tables

Fig. 1. Simplified geological map of the Eastern Pyrenees and the location of the study area.

Fig. 2. Geological map of the study area.

Fig. 3 Synthetic stratigraphy of Lower-to-Middle Paleozoic terrains in the study area and ages of the Middle-Upper Ordovician magmatic rocks obtained in this study. *ages taken from Martínez et al. (2011). The time scale follows Cohen et al. (2013) . The dashed line shows the correlation between the main stratigraphic section at Ribes the Freser (left) and that at Campelles (right).

Fig. 4. Field photographs of the Upper Ordovician magmatic rocks in the study area. A) General view of the Núria gneiss. B) Close-up of the Núria gneiss. C) General view of the Ribes granophyre. D) Close-up of the Ribes granophyre. E) Outcrop of rheomorphic ignimbrites. F) Close-up of the rheomorphic ignimbrites.

Fig. 5U-Pb Wetherill Concordia diagrams of the dated samples. Insets are the $^{206}Pb/^{238}U$ weighted mean dates, normally interpreted as indicative of the crystallization age of the dated samples. In each inset diagram the red lines correspond to the analyses used for mean age calculation; the blue ones in diagrams CAM-12 and CAM-18 are the analyses rejected by the age calculation algorithm in Isoplot 3.7 (Ludwig, 2008). Error bars correspond to 2 sigma errors.

Fig. 6. Diagram of the relative probability with all the inherited zircon grains analysed in this study. The probability plot was produced using Isoplot/Ex 3.7 (Ludwig, 2008). The $^{207}Pb/^{206}Pb$ age was taken for interpretation for all zircons >1.0 Ga, and the $^{206}Pb/^{238}U$ age for younger grains.

Table 1. U-Pb data table

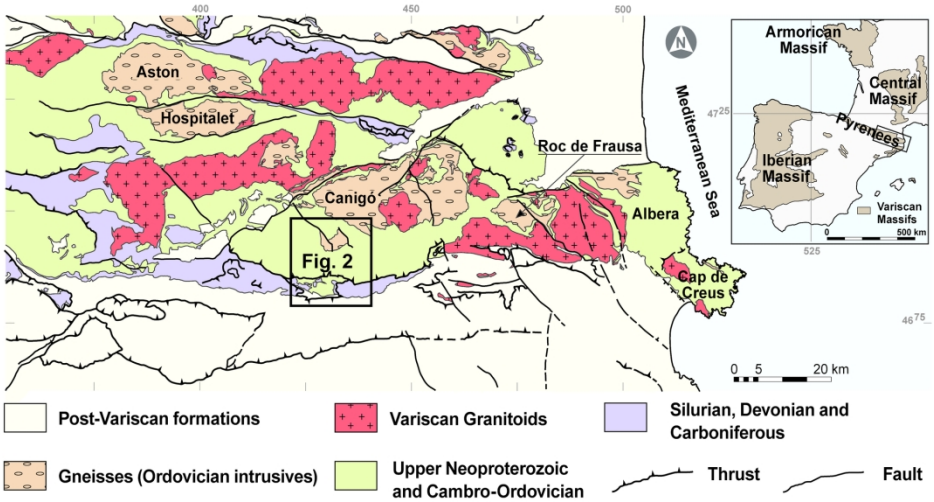

Figure 1. Simplified geological map of the Eastern Pyrenees and the location of the study area.

187x104mm (300 x 300 DPI)

Figure 2. Geological map of the study area.

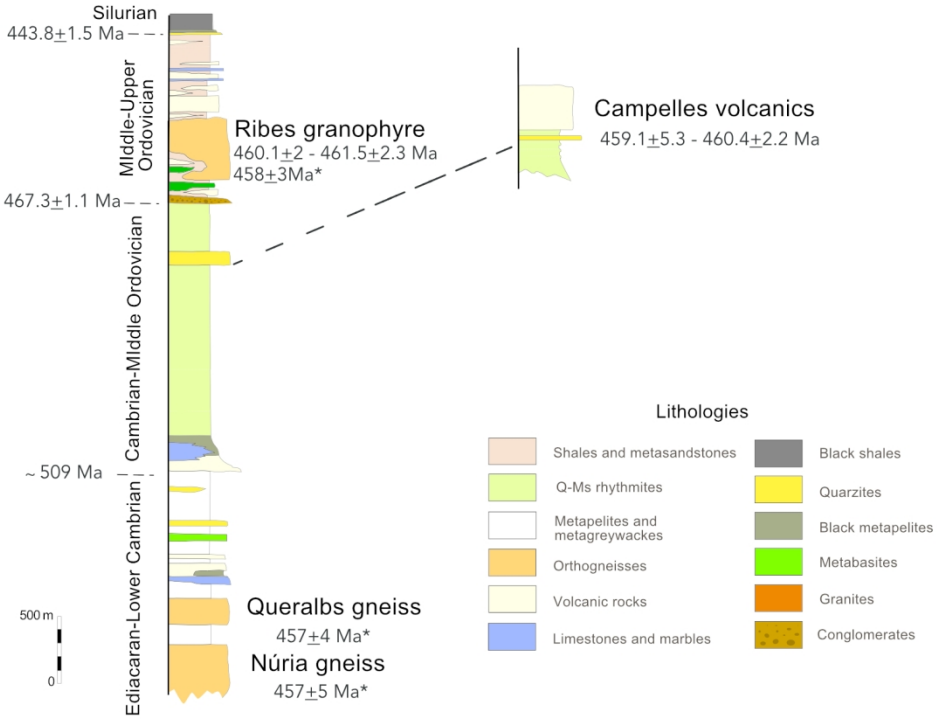

Figure 3. Synthetic stratigraphy of Lower-to-Middle Paleozoic terrains in the study area and ages of the Middle-Upper Ordovician magmatic rocks obtained in this study. *ages taken from Martínez et al. (2011). The time scale follows Cohen et al. (2013) . The dashed line shows the correlation between the main stratigraphic section at Ribes the Freser (left) and that at Campelles (right).

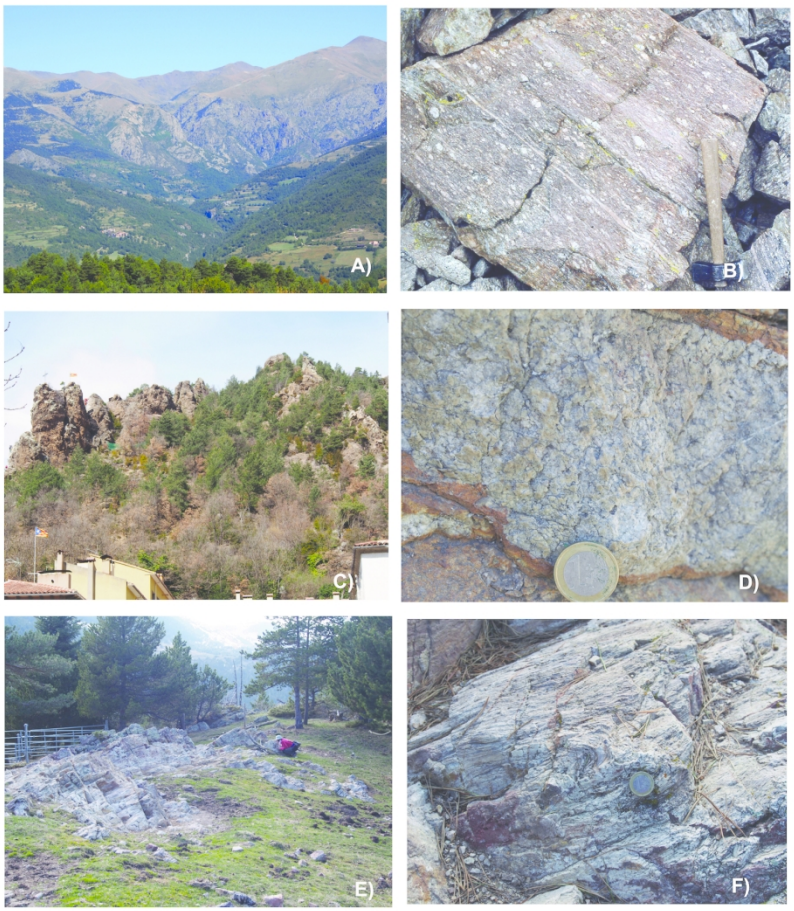

Figure 4. Field photographs of the Upper Ordovician magmatic rocks in the study area. A) General view of the Núria gneiss. B) Close-up of the Núria gneiss. C) General view of the Ribes granophyre. D) Close-up of the Ribes granophyre. E) Outcrop of rheomorphic ignimbrites. F) Close-up of the rheomorphic ignimbrites.

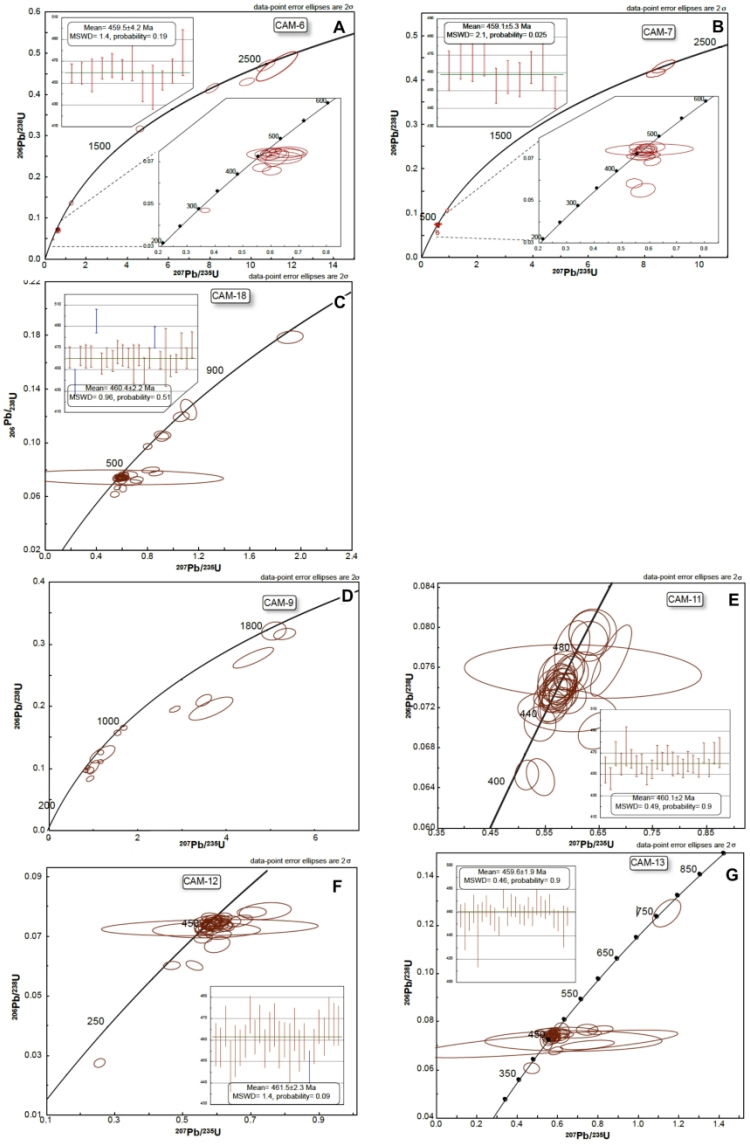

Figure 5. U-Pb Wetherill Concordia diagrams of the dated samples. Insets are the 206Pb/238U weighted mean dates, normally interpreted as indicative of the crystallization age of the dated samples. In each inset diagram the red lines correspond to the analyses used for mean age calculation; the blue ones in diagrams CAM-12 and CAM-18 are the analyses rejected by the age calculation algorithm in Isoplot 3.7 (Ludwig, 2008). Error bars correspond to 2 sigma errors.

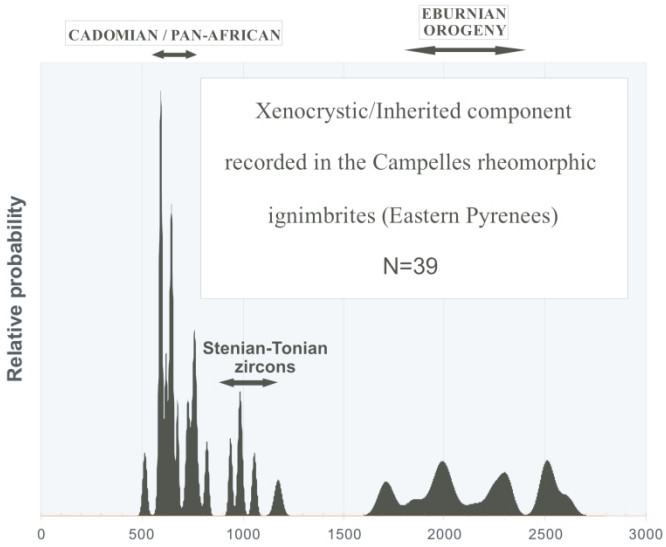

Figure 6. Diagram of the relative probability with all the inherited zircon grains analysed in this study. The probability plot was produced using Isoplot/Ex 3.7 (Ludwig, 2008). The 207Pb/206Pb age was taken for interpretation for all zircons >1.0 Ga, and the 206Pb/238U age for younger grains.

				CORRECTED RATIOS[2]									CORRECTED AGES (Ma)								
	U (ppm)[1]	Th (ppm)[1]	Th/U	$^{207}Pb/^{206}Pb$	±2σ abs	$^{207}Pb/^{235}U$	±2σ abs	$^{206}Pb/^{238}U$	±2σ abs	$^{208}Pb/^{232}Th$	±2σ abs	Rho	$^{206}Pb/^{238}U$	±2σ	$^{207}Pb/^{235}U$	±2σ	$^{207}Pb/^{206}Pb$	±2σ	Best age (Ma)	±2σ	Disc %
Zircon_01_CAM-6	101	47	0.47	0.1057	0.0044	4.6100	0.1600	0.3165	0.0058	0.0965	0.0042	0.05	1772	29	1755	30	1726	75	1726	75	-0.97
Zircon_02_1	383	112	0.29	0.0562	0.0027	0.5720	0.0240	0.0736	0.0014	0.0225	0.0010	0.17	459	9	459	16	440	110	459	9	0.07
Zircon_04_1	694	188	0.27	0.0561	0.0027	0.3660	0.0150	0.0471	0.0009	0.0170	0.0008	0.09	297	5	317	12	460	110	297	5	6.37
Zircon_06_1	217	118	0.54	0.0670	0.0032	0.6040	0.0270	0.0657	0.0016	0.0204	0.0009	0.24	410	10	479	17	820	100	410	10	14.34
Zircon_07_1	126	69	0.55	0.0600	0.0034	0.6190	0.0310	0.0738	0.0017	0.0263	0.0013	0.15	459	10	488	19	600	120	459	10	5.94
Zircon_09_1	201	121	0.60	0.0610	0.0120	0.6190	0.0860	0.0735	0.0024	0.0234	0.0014	0.01	457	15	488	46	680	240	457	15	6.35
Zircon_10_1	133	85	0.64	0.0582	0.0030	0.6040	0.0280	0.0746	0.0016	0.0244	0.0012	0.43	464	10	479	17	520	110	464	10	3.22
Zircon_11_1	108	53	0.49	0.0662	0.0056	0.6730	0.0470	0.0749	0.0018	0.0287	0.0020	-0.17	466	11	525	26	750	130	466	11	11.24
Zircon_12_1	273	148	0.54	0.0624	0.0031	0.5680	0.0270	0.0672	0.0014	0.0222	0.0011	0.06	419	9	456	17	690	110	419	9	8.14
Zircon_13_1	419	376	0.90	0.0580	0.0025	0.5910	0.0230	0.0743	0.0015	0.0226	0.0009	0.40	462	9	471	15	520	94	462	9	1.85
Zircon_14_1	412	200	0.49	0.0740	0.0140	0.7170	0.0410	0.0697	0.0039	0.0243	0.0012	0.15	434	24	547	23	1040	200	434	24	20.66
Zircon_16_1	120	228	1.90	0.0683	0.0035	1.2690	0.0550	0.1363	0.0032	0.0437	0.0016	-0.03	824	18	830	25	890	110	824	18	0.72
Zircon_19_1	169	121	0.72	0.0881	0.0048	0.9270	0.0430	0.0757	0.0029	0.0255	0.0017	0.21	470	18	664	23	1380	110	470	18	29.22
Zircon_20_1	1155	318	0.28	0.1416	0.0053	8.1100	0.2700	0.4153	0.0095	0.1153	0.0049	0.71	2239	44	2243	31	2246	62	2246	62	0.18
Zircon_21_1	93	85	0.91	0.1652	0.0066	10.7100	0.3600	0.4700	0.0110	0.1316	0.0049	0.69	2481	51	2497	33	2506	67	2506	67	0.64
Zircon_22_1	203	98	0.48	0.1643	0.0063	9.8100	0.3000	0.4307	0.0076	0.1292	0.0047	0.44	2309	34	2416	29	2499	64	2499	64	4.43
Zircon_23_1	210	64	0.30	0.0676	0.0036	0.7490	0.0360	0.0801	0.0019	0.0262	0.0015	-0.07	497	11	566	21	830	110	497	11	12.19
Zircon_24_1	50	25	0.50	0.1744	0.0070	11.2500	0.8200	0.4680	0.0290	0.1237	0.0072	0.83	2470	140	2541	91	2609	70	2609	70	2.79
Zircon_25_1	235	76	0.32	0.0623	0.0042	0.6310	0.0650	0.0719	0.0024	0.0265	0.0020	0.03	447	14	500	35	710	140	447	14	10.60
Zircon_26_1	396	321	0.81	0.0644	0.0081	0.6220	0.0350	0.0717	0.0032	0.0229	0.0012	0.50	446	20	496	22	740	180	446	20	10.08
Zircon_27_1	297	205	0.69	0.0607	0.0032	0.5970	0.0270	0.0727	0.0014	0.0234	0.0010	0.03	452	9	474	17	610	110	452	9	4.56
Zircon_28_1	96	51	0.53	0.0640	0.0053	0.6540	0.0500	0.0742	0.0018	0.0232	0.0014	-0.06	461	11	508	29	690	180	461	11	9.25
Zircon_29_1	148	100	0.68	0.0810	0.0110	0.8860	0.0680	0.0769	0.0034	0.0300	0.0017	0.43	478	21	633	34	1340	190	478	21	24.49
Zircon_30_CAM-6	240	179	0.75	0.1678	0.0067	5.9000	0.2100	0.2512	0.0066	0.0545	0.0028	0.74	1444	34	1959	32	2533	65	2533	65	26.29
Zircon_31_CAM-7	207	138	0.67	0.1466	0.0057	8.7000	0.3400	0.4300	0.0120	0.1026	0.0038	0.71	2305	54	2305	35	2303	67	2303	67	0.00
Zircon_33_1	95	13	0.14	0.0628	0.0036	0.9270	0.0470	0.1064	0.0024	0.0273	0.0025	-0.08	652	14	672	25	710	120	652	14	2.98
Zircon_35_1	225	178	0.79	0.0682	0.0035	0.5450	0.0240	0.0584	0.0018	0.0119	0.0007	0.05	366	11	441	16	870	110	366	11	17.01
Zircon_36_1	194	119	0.61	0.0565	0.0026	0.5770	0.0270	0.0742	0.0018	0.0252	0.0012	0.27	461	11	464	17	475	95	461	11	0.65
Zircon_37_1	259	273	1.05	0.0561	0.0031	0.5860	0.0270	0.0750	0.0016	0.0213	0.0009	0.01	466	10	467	17	450	110	466	10	0.19
Zircon_38_1	300	275	0.92	0.0583	0.0028	0.5960	0.0260	0.0751	0.0019	0.0229	0.0011	-0.08	467	12	474	17	530	100	467	12	1.48
Zircon_39_1	196	121	0.62	0.0575	0.0048	0.5920	0.0530	0.0758	0.0022	0.0230	0.0013	0.03	471	13	470	33	500	170	471	13	-0.21
Zircon_40_1	282	249	0.88	0.0641	0.0031	0.6110	0.0250	0.0689	0.0017	0.0182	0.0009	0.32	430	10	488	16	750	110	430	10	11.89
Zircon_41_1	140	110	0.79	0.0748	0.0045	0.5770	0.0360	0.0551	0.0027	0.0141	0.0015	0.27	345	16	461	22	1020	130	345	16	25.16
Zircon_42_1	139	70	0.50	0.0586	0.0041	0.5770	0.0360	0.0713	0.0016	0.0231	0.0013	0.04	444	10	460	23	490	150	444	10	3.46
Zircon_43_1	179	122	0.68	0.0571	0.0034	0.5720	0.0280	0.0727	0.0016	0.0228	0.0012	-0.20	453	10	461	17	490	130	453	10	1.82
Zircon_44_1	136	87	0.64	0.0570	0.0042	0.5780	0.0410	0.0736	0.0015	0.0240	0.0017	-0.03	458	9	462	25	480	140	458	9	0.97
Zircon_45_1	175	96	0.55	0.0581	0.0031	0.5830	0.0270	0.0733	0.0016	0.0238	0.0011	-0.09	456	10	468	18	500	120	456	10	2.54
Zircon_46_1	192	133	0.69	0.0574	0.0032	0.5890	0.0310	0.0744	0.0015	0.0232	0.0010	0.04	463	9	472	19	500	110	463	9	1.97
Zircon_47_1	133	129	0.97	0.1467	0.0059	8.4200	0.2800	0.4154	0.0076	0.1163	0.0042	0.52	2239	35	2276	31	2313	66	2313	66	1.63
Zircon_49_1	402	318	0.79	0.0580	0.0100	0.6000	0.1300	0.0745	0.0022	0.0247	0.0046	0.16	463	13	476	67	530	220	463	13	2.73
Zircon_50_CAM-7	247	150	0.61	0.0582	0.0052	0.5790	0.0500	0.0717	0.0015	0.0222	0.0014	0.25	446	9	463	29	520	160	446	9	3.63
Zircon_51_CAM-9	303	52	0.17	0.1207	0.0054	3.4700	0.1400	0.2092	0.0080	0.1146	0.0076	0.55	1224	43	1519	34	1961	90	1961	90	19.42
Zircon_52_1	311	84	0.27	0.1223	0.0068	4.5800	0.3700	0.2780	0.0130	0.1040	0.0180	0.80	1580	64	1745	58	1987	95	1987	95	9.46
Zircon_53_1	223	57	0.26	0.1336	0.0076	3.6300	0.4100	0.1970	0.0150	0.0292	0.0071	0.75	1158	79	1564	80	2160	110	2160	110	25.96
Zircon_55_1	421	169	0.40	0.1044	0.0041	2.8190	0.0980	0.1951	0.0041	0.0706	0.0025	0.61	1149	23	1360	26	1701	72	1701	72	15.51
Zircon_56	167	202	1.21	0.0720	0.0035	1.5320	0.0640	0.1572	0.0031	0.0470	0.0019	0.11	941	17	947	25	970	100	941	17	0.63
Zircon_57	124	156	1.26	0.0743	0.0035	1.6730	0.0640	0.1656	0.0034	0.0487	0.0020	0.03	988	19	997	26	1034	97	988	19	0.90
Zircon_58	776	157	0.20	0.0708	0.0091	1.2000	0.2300	0.1230	0.0110	0.0370	0.0170	0.69	746	60	801	80	950	180	746	60	6.87
Zircon_59	175	143	0.82	0.1135	0.0059	5.0500	0.2200	0.3210	0.0120	0.0934	0.0042	0.09	1794	61	1827	38	1852	86	1852	86	1.81
Zircon_61	115	105	0.91	0.1224	0.0053	5.2900	0.2000	0.3161	0.0070	0.0931	0.0039	0.23	1770	34	1865	32	1995	75	1995	75	5.09
Zircon_62	326	135	0.41	0.0758	0.0034	1.1660	0.0460	0.1110	0.0021	0.0417	0.0018	0.17	678	12	784	22	1095	88	678	12	13.52
Zircon_63	155	35	0.23	0.0673	0.0036	1.1520	0.0570	0.1258	0.0026	0.0460	0.0022	0.01	764	15	781	27	820	110	764	15	2.18
Zircon_65	162	111	0.69	0.0634	0.0035	0.8190	0.0410	0.0962	0.0021	0.0304	0.0015	0.02	592	13	606	23	690	110	592	13	2.31
Zircon_66	238	219	0.92	0.0627	0.0028	0.8680	0.0320	0.1012	0.0019	0.0312	0.0013	0.01	621	11	633	18	700	100	621	11	1.90
Zircon_67	119	4	0.03	0.0680	0.0051	0.9060	0.0720	0.0974	0.0042	0.0630	0.0120	0.04	599	24	653	28	830	150	599	24	8.27
Zircon_69	979	28	0.03	0.0702	0.0046	0.9880	0.0940	0.1019	0.0095	0.0870	0.0780	0.60	625	53	697	43	940	120	625	53	10.33
Zircon_70	79	62	0.78	0.0783	0.0061	0.9190	0.0640	0.0834	0.0036	0.0302	0.0030	0.51	516	21	663	33	1160	140	516	21	22.17
Zircon_72_CAM-11	406	205	0.50	0.0567	0.0028	0.5670	0.0240	0.0733	0.0014	0.0225	0.0010	0.31	456	9	457	15	460	110	456	9	0.24
Zircon_73	356	160	0.45	0.0576	0.0027	0.5940	0.0240	0.0756	0.0015	0.0248	0.0011	0.30	470	9	473	15	500	100	470	9	0.68
Zircon_74	415	232	0.56	0.0585	0.0025	0.5820	0.0210	0.0733	0.0013	0.0232	0.0009	0.10	456	8	468	14	550	99	456	8	2.61
Zircon_75	187	103	0.55	0.0592	0.0034	0.6120	0.0330	0.0756	0.0016	0.0250	0.0013	0.24	470	10	486	20	560	130	470	10	3.37
Zircon_76	288	205	0.71	0.0590	0.0190	0.6200	0.1800	0.0756	0.0022	0.0240	0.0110	-0.14	470	14	487	83	590	300	470	14	3.49
Zircon_77	768	338	0.44	0.0669	0.0029	0.5760	0.0230	0.0622	0.0011	0.0220	0.0010	0.30	~~389~~	~~7~~	461	15	821	95	389	7	15.62
Zircon_78	234	94	0.40	0.0574	0.0034	0.6380	0.0360	0.0795	0.0019	0.0258	0.0014	0.03	493	11	499	22	470	130	493	11	1.20
Zircon_79	165	79	0.48	0.0552	0.0030	0.5710	0.0280	0.0750	0.0019	0.0245	0.0012	0.19	466	11	457	19	390	120	466	11	-1.97
Zircon_80	377	200	0.53	0.0559	0.0026	0.5770	0.0230	0.0742	0.0014	0.0241	0.0010	0.21	462	8	462	15	467	99	462	8	-0.04
Zircon_81	541	491	0.91	0.0576	0.0026	0.5940	0.0220	0.0754	0.0014	0.0237	0.0009	0.22	468	9	476	14	524	86	468	9	1.62
Zircon_82	304	271	0.89	0.0568	0.0028	0.5770	0.0270	0.0740	0.0018	0.0233	0.0010	0.50	460	11	461	17	470	110	460	11	0.22
Zircon_83	561	396	0.71	0.0560	0.0032	0.5680	0.0320	0.0738	0.0013	0.0225	0.0012	0.57	459	8	456	19	470	110	459	8	-0.64
Zircon_84	375	304	0.81	0.0574	0.0031	0.5760	0.0290	0.0732	0.0014	0.0227	0.0010	0.23	456	9	461	18	490	120	456	9	1.17
Zircon_85	338	163	0.48	0.0565	0.0030	0.5770	0.0250	0.0743	0.0016	0.0218	0.0009	0.24	462	9	462	16	450	120	462	9	0.06
Zircon_86	570	274	0.48	0.0570	0.0024	0.5750	0.0210	0.0739	0.0013	0.0222	0.0009	0.09	459	8	461	13	485	93	459	8	0.35
Zircon_87	443	319	0.72	0.0560	0.0027	0.6000	0.0270	0.0780	0.0022	0.0248	0.0014	0.35	484	13	477	16	450	100	484	13	-1.47
Zircon_88	789	695	0.88	0.0683	0.0039	0.6480	0.0300	0.0697	0.0015	0.0213	0.0010	0.28	435	9	506	19	870	110	435	9	14.13
Zircon_90	585	404	0.69	0.0599	0.0027	0.5410	0.0210	0.0651	0.0015	0.0112	0.0017	-0.27	407	9	439	14	620	100	407	9	7.33
Zircon_91	292	149	0.51	0.0584	0.0030	0.6320	0.0280	0.0786	0.0016	0.0262	0.0012	0.04	488	10	496	18	550	120	488	10	1.71
Zircon_92	356	174	0.49	0.0554	0.0026	0.5630	0.0230	0.0739	0.0015	0.0227	0.0009	0.04	460	9	452	15	430	100	460	9	-1.70
Zircon_93	357	263	0.74	0.0556	0.0028	0.5590	0.0250	0.0721	0.0014	0.0221	0.0009	0.05	449	9	450	16	450	110	449	9	0.29
Zircon_94	185	96	0.52	0.0598	0.0032	0.5920	0.0280	0.0731	0.0014	0.0243	0.0012	0.01	455	9	472	18	570	110	455	9	3.69
Zircon_95	1946	837	0.43	0.0675	0.0027	0.3660	0.0270	0.0394	0.0030	0.0138	0.0012	-0.24	~~249~~	~~18~~	316	19	842	89	249	18	21.20
Zircon_96	463	249	0.54	0.0561	0.0026	0.5780	0.0220	0.0747	0.0014	0.0233	0.0009	0.01	464	9	463	13	454	99	464	9	-0.30
Zircon_97	623	185	0.30	0.0568	0.0027	0.5770	0.0260	0.0735	0.0016	0.0239	0.0013	0.46	457	10	461	17	460	100	457	10	0.78
Zircon_98	702	457	0.65	0.0577	0.0024	0.5160	0.0180	0.0653	0.0012	0.0186	0.0009	0.08	408	7	422	12	511	92	408	7	3.41
Zircon_99	347	236	0.68	0.0551	0.0028	0.5400	0.0240	0.0704	0.0014	0.0219	0.0009	0.00	438	8	438	15	400	120	438	8	-0.09
Zircon_100	622	241	0.39	0.0573	0.0025	0.5690	0.0230	0.0730	0.0020	0.0237	0.0012	0.51	454	12	457	15	493	97	454	12	0.66
Zircon_101	416	354	0.85	0.0598	0.0084	0.5910	0.0750	0.0717	0.0017	0.0215	0.0019	-0.10	446	10	471	39	600	150	446	10	5.31
Zircon_102	121	92	0.76	0.0573	0.0037	0.5880	0.0340	0.0754	0.0018	0.0226	0.0010	0.06	469	11	467	22	500	140	469	11	-0.43
Zircon_103	193	155	0.80	0.0563	0.0030	0.5740	0.0280	0.0739	0.0016	0.0230	0.0009	0.35	460	10	459	17	450	120	460	10	-0.11
Zircon_104	410	227	0.55	0.0646	0.0053	0.6720	0.0310	0.0767	0.0029	0.0281	0.0012	0.79	476	18	521	19	740	140	476	18	8.64
Zircon_105	233	141	0.61	0.0578	0.0032	0.6320	0.0310	0.0795	0.0018	0.0270	0.0012	0.08	493	11	496	19	510	110	493	11	0.60
Zircon_106_CAM-11	499	355	0.71	0.0569	0.0028	0.5690	0.0260	0.0723	0.0014	0.0229	0.0014	0.39	450	8	457	17	480	100	450	8	1.55

Zircon_01_CAM-12	273	123	0.45	0.0554	0.0026	0.5610	0.0220	0.0736	0.0017	0.0246	0.0015	0.28	458	10	454	14	420	100	458	10	-0.88
Zircon_02_2	257	103	0.40	0.0637	0.0033	0.6010	0.0310	0.0672	0.0023	0.0244	0.0013	0.27	~~419~~	~~14~~	477	20	760	110	419	14	12.16
Zircon_03_2	241	157	0.65	0.0603	0.0030	0.6100	0.0280	0.0734	0.0016	0.0250	0.0010	0.13	457	9	482	18	590	110	457	9	5.25
Zircon_04_2	201	131	0.65	0.0591	0.0034	0.6010	0.0290	0.0751	0.0016	0.0244	0.0010	-0.17	467	9	480	17	540	120	467	9	2.79
Zircon_05_2	611	312	0.51	0.0587	0.0026	0.5610	0.0220	0.0694	0.0013	0.0218	0.0009	0.13	~~432~~	~~8~~	452	14	555	99	432	8	4.36
Zircon_06_2	243	137	0.56	0.0630	0.0035	0.6060	0.0310	0.0706	0.0014	0.0224	0.0011	0.06	~~440~~	~~9~~	480	19	670	120	440	9	8.38
Zircon_07_2	705	420	0.60	0.0570	0.0110	0.5700	0.1300	0.0720	0.0021	0.0221	0.0046	0.03	448	12	461	72	500	230	448	12	2.82
Zircon_08_2	289	262	0.91	0.0577	0.0030	0.5880	0.0260	0.0731	0.0021	0.0228	0.0015	0.31	455	12	473	16	520	110	455	12	3.81
Zircon_09_2	636	566	0.89	0.0618	0.0029	0.6230	0.0230	0.0734	0.0014	0.0242	0.0009	-0.11	457	8	491	15	657	94	457	8	7.03
Zircon_10_2	585	370	0.63	0.0564	0.0024	0.5820	0.0210	0.0739	0.0013	0.0237	0.0009	0.26	460	8	465	13	486	88	460	8	1.18
Zircon_11_2	183	126	0.69	0.0704	0.0052	0.7430	0.0620	0.0784	0.0023	0.0256	0.0024	0.24	~~486~~	~~14~~	562	33	920	130	486	14	13.52
Zircon_12_2	239	105	0.44	0.0564	0.0029	0.5860	0.0250	0.0759	0.0015	0.0245	0.0011	-0.25	472	9	467	16	450	120	472	9	-1.01
Zircon_13_2	564	380	0.67	0.0566	0.0024	0.5860	0.0220	0.0742	0.0013	0.0229	0.0009	0.33	461	8	467	14	488	87	461	8	1.20
Zircon_14_2	458	413	0.90	0.0556	0.0027	0.4680	0.0200	0.0602	0.0012	0.0185	0.0007	0.13	~~377~~	~~7~~	389	14	450	100	377	7	3.19
Zircon_15_2	335	86	0.26	0.0586	0.0025	0.6100	0.0220	0.0752	0.0015	0.0277	0.0012	0.08	468	9	483	14	555	91	468	9	3.19
Zircon_16_2	636	509	0.80	0.0568	0.0025	0.5730	0.0220	0.0733	0.0015	0.0236	0.0010	0.33	456	9	460	14	475	96	456	9	0.85
Zircon_17_2	2325	822	0.35	0.0663	0.0030	0.2560	0.0130	0.0276	0.0012	0.0154	0.0008	0.25	~~176~~	~~8~~	232	11	818	95	176	8	24.31
Zircon_18_2	999	928	0.93	0.0640	0.0029	0.5350	0.0200	0.0602	0.0014	0.0180	0.0007	-0.45	~~377~~	~~9~~	434	13	768	91	377	9	13.11
Zircon_19_2	203	82	0.40	0.0655	0.0037	0.7020	0.0350	0.0780	0.0014	0.0306	0.0014	0.06	~~484~~	~~9~~	538	20	810	120	484	9	9.98
Zircon_20_2	226	163	0.72	0.0568	0.0027	0.5850	0.0250	0.0746	0.0015	0.0230	0.0010	0.21	464	9	467	16	480	110	464	9	0.69
Zircon_21_2	446	190	0.43	0.0570	0.0041	0.5860	0.0470	0.0751	0.0017	0.0257	0.0024	0.25	467	10	468	28	490	130	467	10	0.21
Zircon_22_2	157	95	0.61	0.0596	0.0037	0.6030	0.0370	0.0737	0.0019	0.0247	0.0011	-0.03	458	11	480	23	570	130	458	11	4.58
Zircon_23_2	246	107	0.43	0.0584	0.0030	0.5930	0.0260	0.0740	0.0014	0.0245	0.0013	0.03	460	8	472	17	550	110	460	8	2.52
Zircon_24_2	432	189	0.44	0.0590	0.0220	0.5800	0.2600	0.0729	0.0023	0.0230	0.0100	0.21	454	14	470	110	560	320	454	14	3.40
Zircon_25_2	185	142	0.77	0.0611	0.0036	0.6310	0.0330	0.0747	0.0017	0.0240	0.0011	0.20	465	10	499	21	660	120	465	10	6.81
Zircon_26_2	457	285	0.62	0.0568	0.0025	0.5670	0.0240	0.0731	0.0016	0.0232	0.0010	0.45	455	10	457	15	480	96	455	10	0.44
Zircon_27_2	379	131	0.35	0.0585	0.0026	0.5850	0.0250	0.0739	0.0015	0.0235	0.0011	0.24	459	9	469	15	530	100	459	9	2.07
Zircon_28_2	726	544	0.75	0.0564	0.0025	0.5610	0.0210	0.0719	0.0013	0.0225	0.0008	-0.10	448	8	452	13	461	94	448	8	1.00
Zircon_29_2	410	188	0.46	0.0583	0.0035	0.5940	0.0330	0.0735	0.0013	0.0238	0.0015	0.12	457	8	473	20	570	120	457	8	3.38
Zircon_30_1	455	262	0.58	0.0573	0.0025	0.5880	0.0220	0.0750	0.0013	0.0233	0.0009	0.35	466	8	471	14	509	89	466	8	1.00
Zircon_31_1	282	122	0.43	0.0601	0.0031	0.5980	0.0260	0.0742	0.0015	0.0255	0.0012	0.49	462	9	482	18	580	110	462	9	4.21
Zircon_32_2	415	211	0.51	0.0593	0.0027	0.6150	0.0240	0.0757	0.0017	0.0251	0.0011	0.30	470	10	486	15	573	99	470	10	3.29
Zircon_33_2	577	199	0.34	0.0647	0.0034	0.6670	0.0310	0.0752	0.0016	0.0273	0.0011	0.43	467	10	518	19	770	110	467	10	9.77
Zircon_34_2	280	177	0.63	0.0575	0.0029	0.5820	0.0250	0.0751	0.0016	0.0229	0.0010	0.27	467	9	467	16	510	110	467	9	0.06
Zircon_35_CAM-12	693	667	0.96	0.0571	0.0024	0.5660	0.0200	0.0711	0.0013	0.0219	0.0008	0.09	~~443~~	~~8~~	455	13	489	97	443	8	2.70
Zircon_36_CAM-13	155	62	0.40	0.0581	0.0034	0.5790	0.0310	0.0735	0.0016	0.0245	0.0015	0.05	457	10	462	20	510	130	457	10	1.06
Zircon_37_2	134	115	0.86	0.0680	0.0170	0.6800	0.3600	0.0720	0.0034	0.0227	0.0086	0.02	448	20	524	53	860	170	448	20	14.50
Zircon_38_2	521	446	0.86	0.0578	0.0025	0.5850	0.0210	0.0727	0.0014	0.0230	0.0009	0.12	453	8	467	13	530	91	453	8	3.08
Zircon_39_2	291	153	0.53	0.0663	0.0029	1.1420	0.0580	0.1250	0.0048	0.0383	0.0016	0.47	~~759~~	~~28~~	776	30	806	87	759	28	2.19
Zircon_40_2	135	53	0.39	0.0560	0.0032	0.5700	0.0290	0.0745	0.0019	0.0233	0.0012	0.27	463	12	460	19	440	130	463	12	-0.65
Zircon_41_2	299	201	0.67	0.0570	0.0190	0.5500	0.5300	0.0707	0.0046	0.0220	0.0170	0.75	440	27	445	94	510	190	440	27	1.12
Zircon_42_2	247	113	0.46	0.0558	0.0027	0.5740	0.0280	0.0741	0.0014	0.0243	0.0011	0.22	461	8	462	18	440	110	461	8	0.30
Zircon_43_2	215	56	0.26	0.0609	0.0032	0.6240	0.0300	0.0749	0.0015	0.0275	0.0017	0.26	466	9	491	18	610	120	466	9	5.19
Zircon_44_2	272	140	0.51	0.0578	0.0034	0.5830	0.0300	0.0736	0.0014	0.0239	0.0011	-0.28	458	9	465	19	540	120	458	9	1.51
Zircon_45_2	661	617	0.93	0.0772	0.0099	0.7500	0.1100	0.0703	0.0017	0.0200	0.0022	0.49	~~438~~	~~10~~	562	50	1090	190	438	10	22.06
Zircon_46_2	155	84	0.54	0.0578	0.0038	0.5670	0.0330	0.0729	0.0017	0.0250	0.0013	-0.13	454	10	458	21	500	140	454	10	0.87
Zircon_47_2	411	331	0.81	0.0560	0.0027	0.5600	0.0250	0.0720	0.0014	0.0220	0.0009	0.17	448	8	452	16	460	110	448	8	0.84
Zircon_48_2	448	244	0.54	0.0564	0.0025	0.5850	0.0230	0.0758	0.0014	0.0233	0.0009	0.15	472	8	467	15	470	100	472	8	-1.05
Zircon_49_2	593	306	0.52	0.0575	0.0025	0.5780	0.0200	0.0734	0.0013	0.0237	0.0009	0.30	456	8	463	13	512	93	456	8	1.43
Zircon_50_1	475	374	0.79	0.0576	0.0069	0.5840	0.0790	0.0751	0.0016	0.0233	0.0019	-0.21	467	10	466	43	480	200	467	10	-0.11
Zircon_52_2	454	145	0.32	0.0568	0.0026	0.5790	0.0220	0.0748	0.0014	0.0231	0.0010	0.14	465	9	463	14	481	97	465	9	-0.41
Zircon_53_2	595	304	0.51	0.0599	0.0030	0.6170	0.0280	0.0737	0.0014	0.0237	0.0012	0.37	459	8	488	16	590	100	459	8	6.02
Zircon_54_2	473	298	0.63	0.0544	0.0025	0.5530	0.0220	0.0735	0.0014	0.0224	0.0010	-0.11	457	8	447	15	370	100	457	8	-2.30
Zircon_55_2	302	234	0.77	0.0548	0.0028	0.5720	0.0260	0.0746	0.0015	0.0235	0.0009	0.06	464	9	461	16	410	120	464	9	-0.67
Zircon_56_1	423	274	0.65	0.0560	0.0025	0.5700	0.0220	0.0735	0.0014	0.0227	0.0009	0.02	457	8	459	14	442	99	457	8	0.46
Zircon_57_1	340	226	0.66	0.0638	0.0032	0.5930	0.0270	0.0678	0.0014	0.0207	0.0010	0.40	423	8	471	18	710	110	423	8	10.19
Zircon_58_1	183	90	0.49	0.0635	0.0097	0.6600	0.1300	0.0755	0.0018	0.0253	0.0040	-0.07	469	11	508	58	640	220	469	11	7.68
Zircon_59_1	323	226	0.70	0.0568	0.0026	0.5890	0.0230	0.0748	0.0015	0.0234	0.0010	0.13	465	9	470	15	512	98	465	9	1.09
Zircon_60_1	454	346	0.76	0.0557	0.0024	0.5720	0.0210	0.0744	0.0013	0.0236	0.0009	0.08	463	8	459	14	439	94	463	8	-0.76
Zircon_62_1	327	194	0.59	0.0593	0.0030	0.6120	0.0280	0.0751	0.0015	0.0249	0.0010	0.16	467	9	487	17	590	100	467	9	4.15
Zircon_63_1	471	254	0.54	0.0576	0.0027	0.5770	0.0240	0.0731	0.0013	0.0235	0.0009	-0.13	455	8	462	15	490	110	455	8	1.56
Zircon_64_1	254	193	0.76	0.0786	0.0050	0.8150	0.0510	0.0765	0.0015	0.0287	0.0015	0.31	476	9	606	28	1110	130	476	9	21.53
Zircon_65_1	226	118	0.52	0.0602	0.0037	0.6220	0.0310	0.0763	0.0025	0.0249	0.0015	-0.04	474	15	494	20	600	120	474	15	4.05
Zircon_66_1	333	256	0.77	0.0629	0.0030	0.6270	0.0270	0.0728	0.0015	0.0246	0.0010	0.37	453	9	499	15	721	90	453	9	9.28
Zircon_67_1	130	66	0.51	0.0708	0.0043	0.7480	0.0430	0.0767	0.0019	0.0291	0.0015	0.02	476	12	564	25	930	140	476	12	15.60
Zircon_68_1	251	115	0.46	0.0583	0.0044	0.5460	0.0260	0.0719	0.0029	0.0232	0.0021	-0.13	448	18	449	19	500	150	448	18	0.22
Zircon_69_1	485	353	0.73	0.0583	0.0026	0.5890	0.0230	0.0734	0.0013	0.0235	0.0009	0.09	457	8	470	14	540	100	457	8	2.83
Zircon_70_CAM-13	261	749	2.87	0.0567	0.0033	0.4740	0.0320	0.0606	0.0019	0.0153	0.0012	-0.08	~~379~~	~~12~~	393	22	470	120	379	12	3.56
Zircon_71_CAM-18	128	85	0.66	0.0569	0.0042	0.5840	0.0340	0.0741	0.0017	0.0245	0.0012	-0.19	461	10	466	22	480	150	461	10	1.07
Zircon_72_1	234	139	0.59	0.0663	0.0081	0.6500	0.0860	0.0703	0.0019	0.0221	0.0040	0.05	438	12	508	46	800	170	438	12	13.78
Zircon_73_1	306	134	0.44	0.0556	0.0028	0.5700	0.0250	0.0744	0.0015	0.0237	0.0011	-0.14	462	9	457	16	440	110	462	9	-1.18
Zircon_74_1	240	118	0.49	0.0572	0.0039	0.5980	0.0350	0.0744	0.0018	0.0257	0.0012	0.28	462	11	475	21	580	120	462	11	2.74
Zircon_75_1	744	433	0.58	0.0602	0.0025	0.8030	0.0270	0.0972	0.0017	0.0304	0.0011	0.07	~~598~~	~~10~~	598	15	610	93	598	10	0.00
Zircon_76_1	197	61	0.31	0.0593	0.0035	0.5970	0.0290	0.0743	0.0017	0.0240	0.0016	-0.18	462	10	474	18	540	120	462	10	2.53
Zircon_77_1	139	53	0.38	0.0759	0.0052	0.8240	0.0560	0.0799	0.0018	0.0367	0.0024	0.33	495	11	605	31	1060	150	495	11	18.18
Zircon_78_1	247	206	0.83	0.0643	0.0032	0.5470	0.0270	0.0619	0.0018	0.0145	0.0010	0.11	~~387~~	~~11~~	442	17	750	100	387	11	12.44
Zircon_79_1	262	247	0.94	0.0559	0.0033	0.5610	0.0280	0.0732	0.0016	0.0230	0.0010	-0.01	455	10	451	18	410	130	455	10	-0.98
Zircon_80_1	193	111	0.58	0.0569	0.0032	0.5860	0.0300	0.0742	0.0015	0.0236	0.0011	0.00	461	9	467	19	520	120	461	9	1.24
Zircon_81_1	212	93	0.44	0.0625	0.0030	0.6220	0.0260	0.0736	0.0016	0.0236	0.0012	-0.01	458	10	494	16	670	110	458	10	7.33
Zircon_82_1	115	52	0.45	0.0582	0.0042	0.6040	0.0410	0.0750	0.0019	0.0254	0.0014	0.17	466	11	476	26	500	150	466	11	2.10
Zircon_83_1	159	114	0.72	0.0596	0.0032	0.6110	0.0280	0.0744	0.0017	0.0233	0.0011	-0.19	463	10	483	18	580	120	463	10	4.14
Zircon_84_1	332	194	0.58	0.0574	0.0026	0.5860	0.0230	0.0741	0.0014	0.0225	0.0010	0.20	461	9	468	14	500	100	461	9	1.58
Zircon_85_1	211	76	0.36	0.0612	0.0043	0.6040	0.0320	0.0732	0.0030	0.0250	0.0025	0.06	455	18	482	20	650	140	455	18	5.60
Zircon_87_1	156	72	0.46	0.0582	0.0036	0.6040	0.0340	0.0745	0.0016	0.0240	0.0012	-0.02	463	10	478	21	560	140	463	10	3.12
Zircon_88_1	110	48	0.44	0.0713	0.0044	0.7160	0.0410	0.0722	0.0020	0.0266	0.0019	0.14	449	12	550	24	1010	120	449	12	18.36
Zircon_89_1	240	112	0.47	0.0589	0.0035	0.6030	0.0300	0.0741	0.0015	0.0248	0.0011	0.14	461	9	478	19	530	120	461	9	3.66
Zircon_90_1	73	27	0.37	0.0777	0.0039	1.9160	0.0840	0.1786	0.0039	0.0555	0.0032	0.18	~~1059~~	~~21~~	1084	30	1140	100	1059	21	2.31
Zircon_91_1	187	58	0.31	0.0655	0.0034	1.0630	0.0510	0.1195	0.0028	0.0365	0.0020	0.17	~~728~~	~~16~~	746	24	790	110	728	16	2.41
Zircon_92_1	179	89	0.50	0.0827	0.0044	0.8700	0.0440	0.0773	0.0017	0.0346	0.0021	0.33	480	10	636	24	1240	110	480	10	24.53
Zircon_93_1	334	236	0.71	0.0603	0.0028	0.6080	0.0240	0.0737	0.0014	0.0233	0.0010	-0.16	458	8	484	15	599	98	458	8	5.29
Zircon_94_1	151	59	0.39	0.0600	0.0400	0.6000	0.6500	0.0742	0.0046	0.0270	0.0160	-0.16	461	27	470	180	570	420	461	27	1.91
Zircon_95_1	117	34	0.29	0.0645	0.0035	0.9140	0.0420	0.1043	0.0028	0.0347	0.0020	0.10	~~639~~	~~16~~	657	22	740	110	639	16	2.74
Zircon_96_1	181	56	0.31	0.0589	0.0040	0.5840	0.0400	0.0729	0.0017	0.0248	0.0023	0.27	453	10	466	25	530	150	453	10	2.79
Zircon_97_1	276	79	0.29	0.0582	0.0031	0.5860	0.0270	0.0732	0.0014	0.0263	0.0012	0.04	456	8	467	18	540	120	456	8	2.44
Zircon_98_1	222	144	0.65	0.0585	0.0036	0.6150	0.0320	0.0760	0.0020	0.0246	0.0013	0.06	472	12	485	20	530	130	472	12	2.68
Zircon_99_1	103	52	0.50	0.0633	0.0041	0.9210	0.0540	0.1056	0.0024	0.0351	0.0020	-0.10	~~647~~	~~14~~	660	26	710	120	647	14	1.97
Zircon_101_1	228	119	0.52	0.0611	0.0037	0.6170	0.0350	0.0741	0.0016	0.0261	0.0013	0.13	461	10	490	22	640	120	461	10	6.02
Zircon_102_1	227	147	0.65	0.0655	0.0044	1.1220	0.0520	0.1248	0.0063	0.0397	0.0024	-0.38	~~758~~	~~37~~	763	26	780	120	758	37	0.66
Zircon_103_1	331	253	0.76	0.0677	0.0040	0.6080	0.0250	0.0659	0.0022	0.0153	0.0012	0.00	~~411~~	~~14~~	482	16	860	110	411	14	14.73
Zircon_104_1	400	188	0.47	0.0614	0.0027	0.5660	0.0220	0.0664	0.0014	0.0130	0.0008	0.35	~~415~~	~~9~~	455	14	654	96	415	9	8.88
Zircon_105_CAM-18	80	39	0.49	0.0642	0.0051	0.6640	0.0480	0.0761	0.0020	0.0256	0.0013	-0.03	473	12	519	29	710	170	473	12	8.86

1: U and Th concentrations are calculated employing an external standard zircon as in Paton et al., 2010, Geochemistry, Geophysics, Geosystems.
2: 2 sigma uncertainties propagated according to Paton et al., 2010, Geochemistry, Geophysics, Geosystems
$^{207}Pb/^{206}Pb$ ratios, ages and errors are calculated according to Petrus and Kamber, 2012, Geostandards Geoanalytical Research
Analyzed spots were 23 micrometers, using an analytical protocol modified from Solari et al., 2010, Geostandards Geoanalytical Research.
Data measured employing a Thermo iCapQe ICPMS coupled to a Resonetics, Resolution M050 excimer laser workstation.